Computationally efficient modeling of magnetostrictive material based actuator devices

Manik Kumar, Sajan Kumar, Dr. Sushma Santapuri[1]
Department of Applied Mechanics, Indian Institute of Technology Delhi

Abstract: This paper presents a computationally efficient modeling framework for magnetostrictive material based actuator devices. The equations governing the magnetoelastic system include the Navier's equation and the magnetostatic equations coupled through a computationally efficient constitutive model for magnetostrictive materials. The resulting system of nonlinear equations is solved using finite element analysis.

The utility of this framework is demonstrated by applying it to two different actuator geometries: (i) magnetostrictive rod actuator and (ii) cantilevered unimorph beam actuator. The rod actuator is modelled in COMSOL Multiphysics using 2D axisymmetric magnetostriction module whereas the unimorph beam is solved using 1D structural mechanics beam module. Both the models are validated with existing literature. Finally, parametric studies are performed on these actuators under different current and pre-stress conditions to optimize the device performance.

Keywords: Magnetostrictive Materials, Nonlinear Constitutive Modeling, Galfenol, Rod and Beam Actuators.

1 Introduction

Magnetostrictive materials are a class of ferromagnetic materials that exhibit magneto mechanical coupling, i.e., they can stretch in the presence of external magnetic field (Joule effect) or can be magnetized by applying stress (Vilari Effect). These materials have several potential transducer applications like energy harvesting, torque sensing, active vibration control etc. [1, 2]. Materials like Galfenol and Terfenol-D are particularly lucrative due to their unusual ability to produce large magnetostriction strains in the presence of moderate magnetic fields at room temperature. Magnetostrictive material based transducer devices are being developed through a combination of mathematical modeling and experimental characterization. However, owing to the nonlinear and coupled magnetomechanical behavior of these materials, majority of the existing accurate nonlinear models are computationally inefficient and thus are not conducive to device design.

Armstrong [3] formulated a model which uses integration about all possible magnetic moment orientations for calculating bulk magnetization and magnetostriction with an energy-based integral probability density function. In order to improve the computational efficiency, he subsequently restricted the magnetic moment orientation to the eight easy axes of Terfenol-D and used probability density function in discrete form [4]. Atulasimha *et al.* [5] developed a constitutive model for Galfenol by summing the contributions over 98 crystallographic directions as possible orientations. Evan and Dapino [6] proposed a discrete energy averaged (DEA) model for Galfenol by summing over the six easy axes orientations. Computational efficiency was further improved by using a localized form of anisotropy energy defined around each easy axis.

These models were also utilized in design and analysis of magnetostrictive material based transducer devices. Datta *et al.* [7] developed a quasi-static response of the magnetomechanical cantilever for the sensor application. Wun Fogle *et al.* [8] developed a planar magnetomechanical rotation model to predict sensing performance of an amorphous magnetostrictive material adhered to an aluminium cantilever beam and subjected to various loading conditions. More recently, Shu *et al.* [9] utilized the discrete energy-averaged (DEA) model to simulate the 1-D dynamic response of Galfenol-driven unimorph actuators. The DEA model was further utilized by Santapuri *et al.* [10] to model the dynamic response of composite laminate plate actuators with embedded magnetostrictive materials. Computational efficiency of this model was further improved by Tari *et al.* [11].

In this work, a computationally efficient yet accurate constitutive model is adopted [12] for Galfenol which is developed by locally linearizing the total free energy about each easy axis and subsequently utilizing energy averaging techniques to obtain the net magnetization and magnetostriction. This coupled constitutive model is further used for design and analysis of: (i) Galfenol rod actuator and (ii) a unimorph Galfenol-aluminum beam actuator using COMSOL Multiphysics. The results are compared with existing models and experimental results for validation.

This paper is structured as follows: Section 2 presents an overview of our locally linearized magnetomechanical model. Section 3 presents the analysis of a Galfenol rod actuator system actuated by an axial magnetic field. Section 4 presents the formulation and analysis of the unimorph Galfenol-Aluminum cantilevered beam. Finally, the results and contributions of this work are described in Section 5.

2 Modelling of magnetostrictive material medium

2.1 3D magnetomechanical governing equations

Consider a magnetostrictive medium occupying a volume V enclosed by the boundary ∂V and surrounded by free-space V^*. The complete magnetomechanical system is governed by Navier's equation (valid in V), magnetostatic equations, i.e., Gauss's law for magnetism and Ampere's law in the absence of an electric field (Valid in $V \cup V^*$) coupled with magnetomechanical constitutive

[1]Corresponding author. Email: ssantapuri@am.iitd.ac.in; Tel. +91-11-26597393;

equations. Navier's equation in weak form is given by

$$\int_V \left[\mathbf{T}\cdot\delta\,\mathbf{S} + \rho\frac{\partial^2\mathbf{u}}{\partial t^2}\cdot\delta\mathbf{u} + c\frac{\partial\mathbf{u}}{\partial t}\cdot\delta\mathbf{u}\right]dV = \int_{\partial V}\mathbf{t}\cdot\delta\mathbf{u}\,d\partial V + \int_V \mathbf{f}_B\cdot\delta\mathbf{u}\,dV \quad (1)$$

where $\mathbf{T}$ and $\mathbf{f}_B$ denote the stress tensor and and external body force acting on the domain V. The traction vector $\mathbf{t}$ acts on the boundary ∂V. Also, $\mathbf{S}$ and $\mathbf{u}$ are the representations for strain tensor and displacements of each point in the domain V. The strain $\mathbf{S}$ is represented in terms of the displacements $\mathbf{u}$ as

$$\mathbf{S} = \frac{1}{2}\left(\nabla\,\mathbf{u} + \nabla\,\mathbf{u}^{\mathrm{T}}\right). \quad (2)$$

Also, the magnetostatic governing equation in weak form valid in the magnetic material medium and the surrounding free space is given by

$$\int_{\mathcal{E}} \mathrm{grad}\delta\phi\cdot\mathbf{B}\,dV = 0 \quad (3)$$

where ϕ is the magnetic scalar potential, related to the magnetic field $\mathbf{H}$ as $-\mathrm{grad}\,\phi = \mathbf{H}$. Also, $\mathcal{E} \equiv V \cup V^*$ represents the Euclidean space $\mathcal{R}^3$ consisting of the Galfenol actuator setup and the surrounding free-space. Also, the nonlinear constitutive relations for stress and magnetic flux in the form

$$\mathbf{T} = \mathbf{C}(\mathbf{S} - \boldsymbol{\lambda}(\mathbf{T},\mathbf{H})), \quad \mathbf{B} = \mu_o(\mathbf{H} + \mathbf{M}(\mathbf{T},\mathbf{H})) \quad (4)$$

where, $\mathbf{C}$ is the compliance matrix, $\boldsymbol{\lambda}(\mathbf{T},\mathbf{H})$ and $\mathbf{M}(\mathbf{T},\mathbf{H})$ represent the magnetostriction tensor and magnetization vector obtained from the computationally efficient constitutive model developed in next subsection.

2.2 Overview of the magnetomechanical constitutive model for single crystal Galfenol

Finite element implementation of transducer devices made of complex materials like Galfenol with inherent nonlinearities and coupling (as described by Eq.(4)), often result in computationally inefficient models that are not conducive to device design. In this work, a novel computationally efficient nonlinear model for Galfenol is utilized to enable faster computational device design and analysis [12]. Parameters taken for constitutive relation is listed in table (1). An overview of this model is presented below.

Magnetostrictive material models are traditionally developed through constrained energy minimization [2, 13, 3]. The objective function is the constrained free energy

$$\psi_{cons}(m_1,m_2,m_3,L) = \psi_{anisotropy} + \psi_{zeeman} + \psi_{magnetoelastic} + L(m_1^2+m_2^2+m_3^2-1) \quad (5)$$

where, m_1, m_2 and m_3 represent the Cartesian components of the magnetic moment orientation $\mathbf{m}$ such that $|\mathbf{m}| = m_1^2+m_2^2+m_3^2 = 1$ and L is the Lagrange multiplier. The energy term $\psi_{anisotropy}$ represents the magnetic anisotropy energy defined (for a cubic crystal structure) by

$$\psi_{anisotropy} = K_1(m_1^2m_2^2 + m_2^2m_3^2 + m_3^2m_1^2) + K_2m_1^2m_2^2m_3^2 \quad (6)$$

where K_1 and K_2 are the cubic anisotropy constants. ψ_{zeeman}, i.e., the Zeeman energy is the energy due to the applied/external magnetic field given by

$$\psi_{zeeman} = -\mu_0M_s(H_1m_1 + H_2m_2 + H_3m_3) \quad (7)$$

where H_1, H_2 and H_3 are the scalar components of the applied magnetic field along [100], [010], and [001] crystal directions, respectively. μ_o is the permeability of free-space (universal constant) and M_s is the saturation magnetization (a material constant). $\psi_{magnetoelastic}$, i.e., the energy due to magnetomechanical interactions within the material is given by

$$\psi_{magnetoelastic} = -\gamma^\sigma\frac{3}{2}\lambda_{100}\left(m_1{}^2T_1 + m_2{}^2T_2 + m_3{}^2T_3\right) - 3\gamma^\sigma\lambda_{111}\left(m_1m_2T_4 + m_2m_3T_5 + m_3m_1T_6\right) \quad (8)$$

where λ_{100} and λ_{111} are the magnetostriction constants in $<100>$ and $<111>$ directions, respectively. Also, the constant γ^σ is a scaling parameter which has been used in the literature previously (for instance, see Atulsimha *et al.* [2]).

In order to improve the computational efficiency of the model, we perform a Taylor series expansion (up to degree 2) of the objective function (5) about the easy axes. We now specialize to Galfenol that has 6 mutually independent easy axes orientations along $<100>$.

Let $\mathbf{c}^k$ denote the unit vector along the k^{th} easy axis (k = 1,2,..6). Taylor series expansion of the objective function about each $\mathbf{c}^k$ (truncated at degree 2) is given by

$$\psi^k_{cons} = \psi_{cons}\Big|_{\boldsymbol{c^k}} + \frac{\partial\psi^k_{cons}}{\partial m^k_i}\Big|_{\boldsymbol{c^k}}(m^k_i - c^k_i) + \frac{1}{2}\frac{\partial^2\psi_{cons}}{\partial m_im_j}\Big|_{\boldsymbol{c^k}}(m^k_i - c^k_i)(m^k_j - c^k_j) + \frac{\partial\psi_{cons}}{\partial L}\Big|_{\boldsymbol{c^k}}$$

where ψ^k_{cons} and $\mathbf{m}^k$ denote the local objective function and magnetic moment orientations defined in the kth domain. Noting that $\frac{\partial\psi^k_{cons}}{\partial L}\Big|_{\boldsymbol{c^k}} = 0$, we obtain the local magnetic moment orientations using

$$\frac{\partial\psi^k_{cons}}{\partial m^k_i} = \frac{\partial\psi^k_{cons}}{\partial m^k_i}\Big|_{\boldsymbol{c^k}} + \frac{\partial^2\psi^k_{cons}}{\partial m^k_im^k_j}\Big|_{\boldsymbol{c^k}}(m^k_j - c^k_j) = 0 \quad (9)$$

We simplify further by specializing to Galfenol wherein $c^k_ic^k_j = 0$ for $i \neq j$. Equation (9) is solved to obtain the magnetic moment orientations $\boldsymbol{m}^k$ that minimize the energy around the kth axis. The optimization problem is further simplified by linearizing the constraint $\mathbf{m}\cdot\mathbf{m} \approx \mathbf{m}\cdot\mathbf{c} = 1$. Thus the solution to (9) is reduced to the form

$$[\tilde{\boldsymbol{K}}^k][\boldsymbol{m}^k - \boldsymbol{c}^k] = [\boldsymbol{B}^k], \quad (10)$$

where $\boldsymbol{B}^k$ vector and modified $\tilde{\boldsymbol{K}}^k$ matrix elements can be written as:

$$[\boldsymbol{B}^k] = \begin{bmatrix} \mu_0 M_s H_1(1-{c_1}^2) + [3\lambda_{100} c_1 T_1(1-{c_1}^2) + 3\lambda_{111}(c_2 T_4 + c_3 T_6)] \\ \mu_0 M_s H_2(1-{c_2}^2) + [3\lambda_{100} c_2 T_2(1-{c_2}^2) + 3\lambda_{111}(c_1 T_4 + c_3 T_5)] \\ \mu_0 M_s H_3(1-{c_3}^2) + [3\lambda_{100} c_3 T_3(1-{c_3}^2) + 3\lambda_{111}(c_1 T_6 + c_2 T_5)] \end{bmatrix}$$

$$K_{ij}^k = \left\{ \begin{array}{cc} 2K(1-c_i^2+c_i) + 3\lambda_{100} T_{ii}(c_i^2-1), & i=j(\text{no sum}) \\ 3\lambda_{111} T_{ij}(c_i^2-1) + 2Kc_j, & i \neq j \end{array} \right\}$$

In order to maintain the stability of the model without sacrificing its efficiency in all direction, $\boldsymbol{m}^k$ is normalized as done by [14] and used as normalized $\tilde{\boldsymbol{m}}^k$ in all future calculations.

$$\tilde{\boldsymbol{m}}^k = \frac{\boldsymbol{m}^k}{\| \boldsymbol{m}^k \|} \tag{11}$$

The model can sometimes result in singularity error which is corrected by adding the modified constraint $\mathbf{m}^k \cdot \mathbf{c}^k = 1$ in the form

$$2K[c_1(m_1-c_1) + c_2(m_2-c_2) + c_3(m_3-c_3)] = 0$$

to each equation which in turn removes the singularity in the problem.

Therefore, bulk magnetization **M** can be calculated by summing magnetic moment orientations over all domains

$$\mathbf{M} = M_s \mathbf{m} = M_s \sum_k \overset{k}{\xi}_{an} \overset{k}{\tilde{\mathbf{m}}} \tag{12}$$

where M_s represents saturation magnetization, $\overset{k}{\xi}_{an}$ is the anhysteretic volume fraction of the kth domain defined by

$$\overset{k}{\xi}_{an} = \frac{exp(\frac{-\psi^k}{\omega})}{\sum_{k=1}^{r} exp(\frac{-\psi^k}{\omega})}$$

where, ω is the smoothing constant. The corresponding magnetic flux density **B** can be calculated as

$$\mathbf{B} = \mu_o(\mathbf{H}+\mathbf{M}) = \mu_o(\mathbf{H} + M_s \sum_k \overset{k}{\xi}_{an} \overset{k}{\mathbf{m}}) \tag{13}$$

Table 1: Material parameters selected for Galfenol

Parameters	Name	Numerical Value	Unit
$(3/2)\lambda_{100}$	Magnetostrictive constant	255×10^{-6}	–
$(3/2)\lambda_{111}$	Magnetostrictive constant	-7×10^{-6}	–
μ_0	Vacuum Permeability	$4\pi \times 10^{-7}$	Hm^{-1}
M_s	Saturation Magnetization	$1.83/\mu_0$	Am^{-1}
K_1,K_2	Anisotropy Coefficient	3.6×10^4,0	Jm^{-3}
Ω	Smoothing Constant	625	Jm^{-3}
γ^σ	Fit Constant	0.8	–

3 2-D axisymmetric rod actuator

In this section, magnetomechanical modeling of Galfenol rod actuator using COMSOL Multiphysics version 5.3a. The magnetostrictive rod system is solved using the 2D axisymmetric stress-strain static analysis and 2D axisymmetric magnetostatics interface coupled through our locally linearized magnetomechanical constitutive model. Solution procedure utilized in this work is described in Figure 1.

Actuator Geometry: The rod actuator set-up is described in Figure 2 consists of a cylindrical Galfenol rod actuator of length 50 mm and 6 mm diameter, an axisymmetrically wound current carrying coil inductor (which induces magnetic field into the material), steel casing to provide flux return path and the surrounding air domain (approximated as free space) sufficiently large to ensure zero magnetic pontetial at its outermost boundary. Also, the bottom end of the rod is kept fixed, and the top end is free to move.

Simulations results are verified against the COMSOL Multiphysics built-in model (nonlinear magnetostrictive transducer).

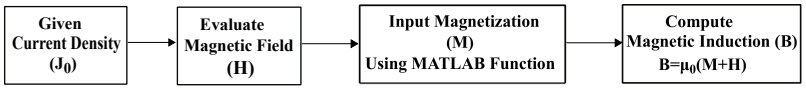

Figure 1: Block diagram of coupled magnetoelastic model embedded in COMSOL

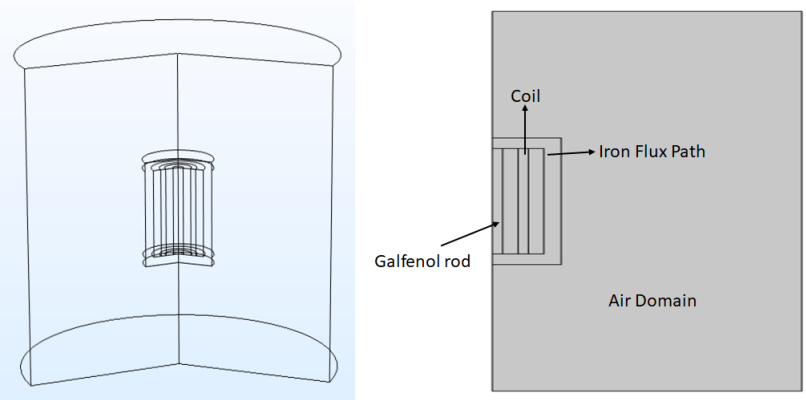

Figure 2: Schematic diagram of Galfenol rod actuator

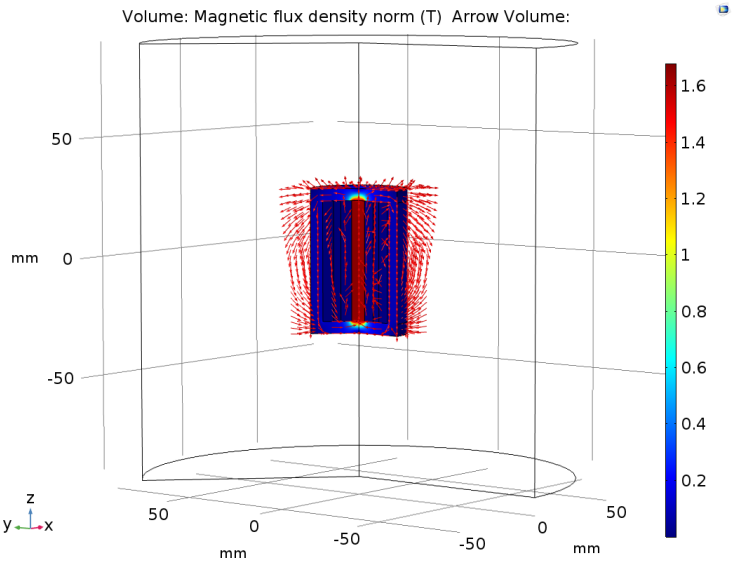

Figure 3: 3D of the norm of magnetic flux density

3.1 Simulation results

The COMSOL model is utilized to calculate magnetic flux density and magnetostriction in the Galfenol rod for different coil current inputs.

Figure 3 illustrates the output magnetic flux density for an input coil current density J_0=1$\times 10^7$ A/m^2. We observe an approximately uniform magnetic flux density ($\approx$ 1.6 T) in the Galfenol rod. The closed iron flux path around the Galfenol rod reduces leakage by allowing majority of the magnetic flux lines to pass through it.

Furthermore, parametric studies are performed to obtain characteristic λ-J_0 and B-J_0 plots at various pre-stress (uniform compressive stress along the axis of the rod) and coil current density values as illustrated in Figure 4.

As expected, an increase in input current density (at zero pre-stress) leads to increase in magnetostriction and magnetic flux density until the saturation wherein all the magnetic moments orient along the axis of the rod (aligned with magnetic field direction). However, with the increase in pre-stress values magnetic moments tend to orient in a direction perpendicular to applied stress. Thus, it is observed that for nonzero pre-stress values higher magnetic fields are required to magnetize the material (i.e., slower saturation) which in turn leads to larger magnetostriction. Saturation is observed at a current density $J_0 \geq 1500$ kA/m^2 wherein all the moments are fully aligned with the magnetic field direction, i.e., the Galfenol rod is fully magnetized. Furthermore, we observe that the maximum value of saturation magnetostriction is 170.2 ppm for zero pre-stress and 255 ppm for all other pre-stress values.

4 Composite unimorph bending actuator

In this section, a unimorph cantilevered beam actuator is analyzed using the Euler-Bernoulli beam theory along with our locally linearized constitutive model. Here a uniform axial magnetic field is assumed to be generated from a coil wound around the beam and is calculated using $H = NI$, where I is the input current, N is the coil constant and H is the magnitude of applied magnetic field. Furthermore, it is assumed that the change in magnetic field caused by deformation of the beam is negligible.

Actuator Geometry: The unimorph cantilevered bending actuator set-up described in Figure 5 consists of a Galfenol-aluminum composite beam of length 82 mm and width 9 mm and thickness 5.66 mm (t_g = 1.83 mm and t_s = 3.83 mm) are measured along x, y and z-axis respectively. The unimorph is subjected to quasi-static magnetic field along its longitudinal axis. Simulations are carried out in COMSOL by performing the structural analysis of composite unimorph using the 1D beam structural mechanics module. Parameter taken for aluminium and Galfenol is listed in table 2. Results are discussed in subsequent sections.

Table 2: Parameters used in the composite unimorph bending actuator

Parameters/Materials	Galfenol	Aluminum
$\rho(kg/m^3)$	7870	2700
E (GPa)	63	70
ν	0.45	0.33

4.1 Derivation on the 1D weak form

In order to derive the weak form of our Euler-Bernoulli beam governing equations, we define the displacement vector $\mathbf{u} = \begin{Bmatrix} u_x \\ u_y \end{Bmatrix}$ where u_x and u_y represent the x and y components of the displacement vector.

where the standard displacement assumptions of the Euler-Bernoulli beam theory (as shown in Figure 5) are used, i.e.,

$$u_x(x,y) = u_0(x) - y\frac{du_y}{dx} \quad u_y(x,y) = u_y(x)$$

The normal strain along the axis, i.e., ε_{xx} is given by

$$\varepsilon_{xx} = \frac{\partial u_x}{\partial x} = \varepsilon_0 - y\frac{d^2u_y}{dx^2} = \varepsilon_0 - y\kappa$$

where ε_0 is the mid-plane strain of the composite beam and κ is the curvature of the beam about the z-axis.

The stress-strain relationships in the Galfenol and aluminum layers are given by

$$\sigma_{xx} = E_g(\varepsilon_0 - y\kappa - \lambda) \qquad \text{(Galfenol)} \tag{14}$$
$$\sigma_{xx} = E_s(\varepsilon_0 - y\kappa) \qquad \text{(Aluminum Substrate)} \tag{15}$$

We now define the resultant force N and the resultant moment M as follows:

$$N = \int_0^b \int_{-t_s}^{t_g} \sigma_{xx} dydz, M = \int_0^b \int_{-t_s}^{t_g} y\sigma_{xx} dydz \tag{16}$$

These expressions are further simplified by substituting the constitutive relationships (14) - (15) into (16) and integrating to obtain the following reduced expressions. After integration above form of N and M can be rewritten

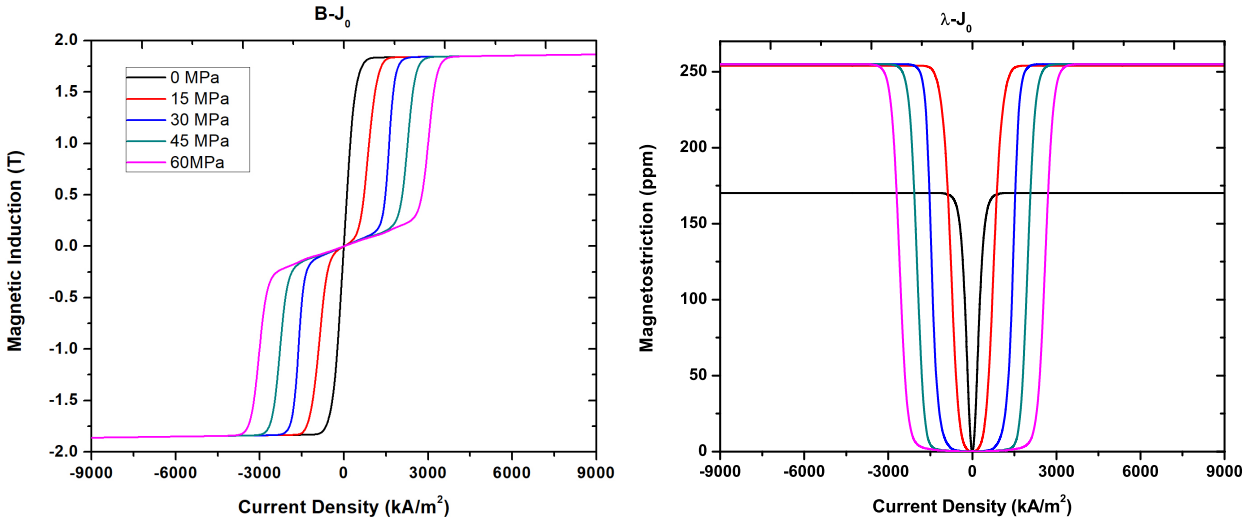

Figure 4: Actuator characteristics along axial direction for various pre-stress values

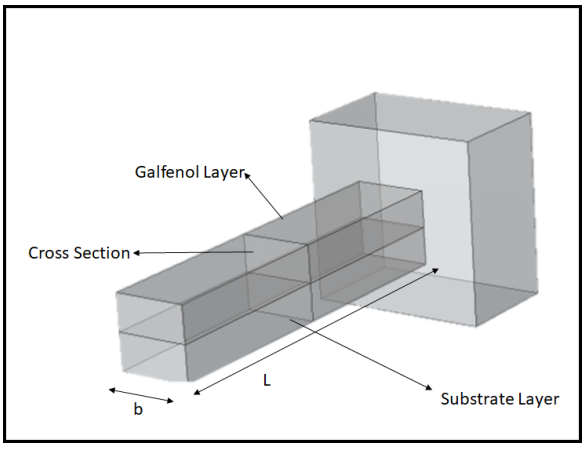

Figure 5: Galfenol-Aluminium laminated composite cantilever unimorph

as

$$\begin{Bmatrix} N \\ M \end{Bmatrix} = \begin{bmatrix} E_{\text{effective}} A_{\text{effective}} & b(E_s \frac{t_s^2}{2} - E_g \frac{t_g^2}{2}) \\ b(E_s \frac{t_s^2}{2} - E_g \frac{t_g^2}{2}) & E_{\text{effective}} I_{\text{effective}} \end{bmatrix} \begin{Bmatrix} \varepsilon_0 \\ \kappa \end{Bmatrix} + \begin{Bmatrix} -E_g A_g \lambda \\ E_g b \frac{t_g^2}{2} \lambda \end{Bmatrix} \quad (17)$$

Where

$$E_{\text{effective}} = \frac{(E_g A_g + E_s A_s)}{(A_g + A_s)}, \quad A_{\text{effective}} = A_g + A_s,$$

and

$$I_{\text{effective}} = I_g + I_s + A_g(\frac{t_g}{2})^2 + A_s(\frac{t_s}{2})^2$$

.

Finally, the variational form (1) can be reduced to the following 1D form

$$\int_0^L (\frac{d\delta u_x}{dx} N - \frac{d^2 \delta u_y}{dx^2} M) dx = \int_0^L (\delta u_x p_x + \delta u_y p_y) dx \quad (18)$$

for a catilevered beam deforming under the external loads p_x and p_y (forces per unit length) acting along x and y axes, respectively. Also, δu_x and δu_y represent the x and y components of the variational displacement $\delta \mathbf{u}$. Expression (17) along with the $\lambda - H$ constitutive relationship developed in Section 2 is fed through MATLAB LIVELINK into COMSOL beam formulation. In our case, the beam is subjected to only magnetic field, so all expression on the right side of equation (18) reduce to zero. The simulations results are discussed in the subsequent section.

4.2 Simulation results

The 1D beam model developed in COMSOL is utilized to calculate tip displacement, bending strain ε_{xx} in Galfenol and Aluminum substrate layers with varying thickness ratio ($t_r = t_g/t_s$) and magnetic field values, respectively. The results agree well with the model presented by Datta *et al.* [7].

Effect of thickness ratio on normalized tip displacement

Tip displacement of the unimorph beam is studied as a function of varying Galfenol-to-substrate thickness ratio t_r. The results in Figure 6 show the existence of a critical thickness ratio beyond which the tip displacements decrease with increasing thickness ratio. The tip displacement is thus increasing with Galfenol volume fraction up to the critical thickness ratio and the Galfenol sheet's offset from the neutral axis. As the sheet's thickness increases above the critical value, the neutral axis moves within the sheet, thus reducing the bending displacement.

Effect of the passive layer thickness

Normal strain ε_{xx} at the top of Galfenol layer and at the bottom of aluminum layer for varying magnetic field and substrate thicknesses is illustrated in Figure 7. For a constant aluminium thickness, strain in Galfenol layer increases monotonically with the increase in the magnetic field till saturation is reached as shown in Figure 7(a). However, saturation strain increases with a decrease in aluminium layer thickness.

Strain on aluminium surface as a function of varying magnetic field and substrate thickness is plotted in Figure 7(b). In general, the magnitude of strain increases with the increase in magnetic field until saturation. Furthermore, at a substrate thickness of 0.46 mm, a positive strain is observed at all magnetic field values. However, as the aluminium thickness increases, i.e., at t_s =0.85 mm, 3.71 mm, and 7.43 mm, strain is largely compressive and increases in magnitude with increasing magnetic field. This can be explained by the fact that bending effect becomes predominant compared to extension as the substrate thickness increases.

5 Conclusion

A computationally efficient mathematical modeling framework was developed for magnetostrictive material-based transducer devices. A novel locally linearized anhysteretic model was integrated with magnetostrictive module in COMSOL Multiphysics 5.3a to study two different Galfenol actuator geometries, namely, a Galfenol rod actuator and a Galfenol-aluminum composite beam actuator.

The results obtained for the rod actuator were validated using the COMSOL Multiphysics in-built model name as Nonlinear Magnetostrictive Transducer. It was further observed that the maximum value of saturation magnetostriction is 170.2 ppm for zero pre-stress and 255 ppm for all other pre-stress values.

An extended Euler-Bernoulli beam theory was used for analysis of the composite Galfenol-aluminum beam actuator. The results agreed well with the experimental and computational data presented in Datta *et al.*[7]. Parametric studies were performed for different Galfenol to substrate thickness ratios and the strains in both the layers were studied for different pre-stress values. It was observed that the tip displacement was maximized at a critical thickness ratio of around 2. Also, it was seen that for very small substrate thickness, the strain in this layer was mainly extensional. However, with increase in thickness, bending strains became predominant.

References

[1] L. Sallese, A. Scippa, N. Grossi, G. Campatelli, Investigating actuation strategies in active fixtures for chatter suppression, Procedia CIRP 46 (2016) 311–314.

[2] J. Atulasima, A. B. Flatau, J. R. Cullen, Energy-based quasi-static modeling of the actuation and

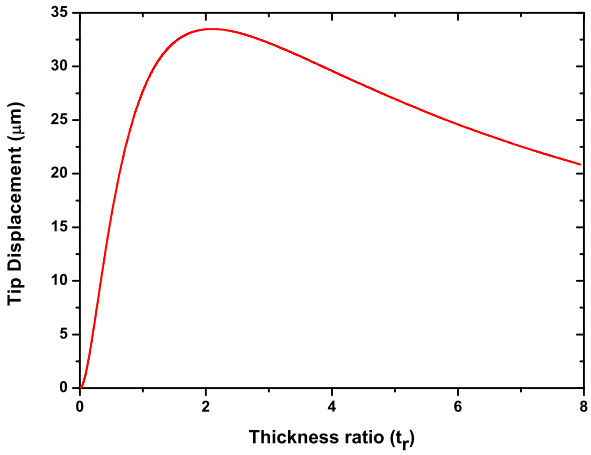

Figure 6: Tip displacement of Galfenol-Alumnium cantilevered unimorph

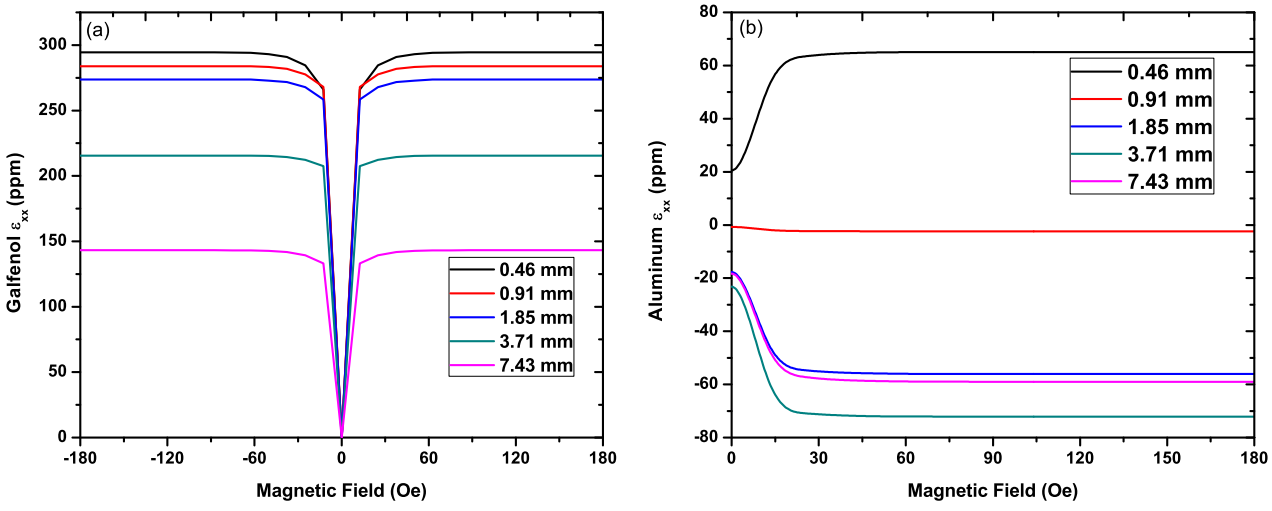

Figure 7: Free strain (ε_{xx}) on (a) Galfenol surface (b) Aluminum (substrate) surface as a function of applied magnetic field for different substrate thicknesses.

sensing behavior of single-crystal iron-gallium alloys, Journal of Applied Physics 103 (1) (2008) 014901.

[3] W. D. Armstrong, Magnetization and magnetostriction processes in tb (0.27- 0.30) dy (0.73- 0.70) fe (1.9- 2.0), Journal of Applied Physics 81 (5) (1997) 2321–2326.

[4] W. D. Armstrong, An incremental theory of magneto-elastic hysteresis in pseudo-cubic ferromagnetostrictive alloys, Journal of Magnetism and Magnetic Materials 263 (1-2) (2003) 208–218.

[5] J. Atulasimha, G. Akhras, A. B. Flatau, Comprehensive three dimensional hysteretic magnetomechanical model and its validation with experimental $<$ 110 $>$ single-crystal iron-gallium behavior, Journal of Applied Physics 103 (7) (2008) 07B336.

[6] P. Evans, M. Dapino, Efficient magnetic hysteresis model for field and stress application in magnetostrictive galfenol, Journal of Applied Physics 107 (6) (2010) 063906.

[7] S. Datta, J. Atulasimha, C. Mudivarthi, A. B. Flatau, Modeling of magnetomechanical actuators in laminated structures, Journal of Intelligent Material Systems and Structures 20 (9) (2009) 1121–1135.

[8] M. Wun-Fogle, H. T. Savage, A. E. Clark, Sensitive, wide frequency range magnetostrictive strain gage, Sensors and Actuators 12 (4) (1987) 323–331.

[9] L. Shu, L. M. Headings, M. J. Dapino, D. Chen, Q. Lu, Nonlinear model for galfenol cantilevered unimorphs considering full magnetoelastic coupling, Journal of Intelligent Material Systems and Structures 25 (2) (2014) 187–203.

[10] S. Santapuri, J. Scheidler, M. Dapino, Two-dimensional dynamic model for composite laminates with embedded magnetostrictive materials, Composite Structures 132 (2015) 737–745.

[11] H. Tari, S. S. Santapuri, M. J. Dapino, Efficient and robust nonlinear model for smart materials with application to composite magnetostrictive plates, Smart Materials and Structures 26 (4) (2017) 045010.

[12] S. Kumar, M. Kumar, S. Santapuri, A computationally efficient energy-averaged constitutive model for magnetostrictive materials, (**In Preparation**).

[13] D. C. Jiles, D. L. Atherton, Theory of ferromagnetic hysteresis, Journal of applied physics 55 (6) (1984) 2115–2120.

[14] S. Chakrabarti, Modeling of 3d magnetostrictive systems with application to galfenol and terfenol-d transducers, Ph.D. thesis, The Ohio State University (2011).